

AIRBAG DEPLOYMENT FOR PROTECTION OF DISABLED AIRCRAFT AND HELICOPTERS OPERATING AT SEA

Xavier J. R. Avula*, **Narendra Guraju♦**, and **Satyakishore Renduchintala***

Department of Mechanical and Aerospace Engineering and Engineering Mechanics
University of Missouri-Rolla, Rolla, Missouri 65409-0050 U.S.A.

ABSTRACT

In the present study, the possibility of using airbags as protective devices for disabled aircraft and helicopters operating at sea is considered. A computer simulation of the deployment of an initially folded airbag and its impact with a water surface is performed using the nonlinear finite element program LS-DYNA3D. When the airbag is inflated from different initial positions above the water surface, practically no difference in the unfolding timings of airbag is observed from the timings of the airbag deployed without water surface. When an airbag is attached to the base of a freely falling body such as a disabled helicopter and deployed against the water surface, there exists an optimal distance from which the airbag has to be deployed against the water surface for highest protection. A parametric study is conducted to investigate the influence of airbag parameters on the evolution of pressure, volume and temperature within the airbag when it is inflated against the water surface. Various airbag parameters including venting, fabric density, fabric elasticity and input gas temperature are considered. It is observed that low input gas temperature resulted in improper inflation of the airbag. Higher fabric densities significantly increased the ability of airbag to withstand higher pressures. Also, it is inferred that higher bag elasticities are required to make stiff material bags which can withstand higher pressures involved in helicopter crashes. Though the ability of the bags to withstand higher pressures is an important criteria, the chief purpose of an airbag is to prevent injury to the occupants and damage to the structure during a crash. So a recommendation is made to strike a balance between various airbag parameters such that airbag could withstand higher pressures and at the same time should offer less rebound to the structure and the occupants.

I. INTRODUCTION

Innovative design concepts have made modern military aircraft crashworthy. Energy absorbing seat design and break-away components of the cockpit interior have resulted in fewer injuries due to impact accelerations. Despite significant advances in accident prevention, crashworthiness, and individual protective equipment, head and torso injuries due to flailing have continued to cause death and disability in survivable military helicopter accidents. A study of U.S. helicopter crashes by Coltman et al., [1] to quantify the impact parameters and identify hazards causing injuries and fatalities revealed that of one hundred and eighty six mishaps in a ten-year period (1972-1981), one hundred and fifty four were judged survivable. The use of supplemental inflatable restraint systems, which has been applied to reduce injuries in automobiles by minimizing occupant motion and subsequent collision with the vehicle's interior, has been extended to Army

* Professor Emeritus ♦ Former Graduate Student ♣ Graduate Student

helicopters and its effectiveness demonstrated by the U.S. Army Aeromedical Research Laboratory. Alem et al. [2] and Shanahan et al. [3] have addressed the issue of airbags for aviation safety and concluded that an airbag system, specifically designed for a helicopter, could significantly reduce severe head and chest injuries and fatalities. Numerous other issues of airbags for aviation safety were addressed at the Technical Cooperative Program Workshop on Inflatable Restraints in Aviation [4].

With the advent of widespread use of airbags for protection in automobile crashes, the use of computer simulation techniques in crash safety design has rapidly increased. The study of an inflatable restraint system includes consideration of various airbag materials, physical parameters that affect the inflation of the airbag, folding patterns, deployment patterns with different types of occupant bodies and finally, interaction with the entire occupant model. Several finite element models for the simulation of airbag deployment and its interaction with occupant model have been developed. Modeling the airbag by the finite element formulation allows one to determine the topological characteristics of the airbag and its contact with the impacting object with greater accuracy at any time during the simulation. Improved accuracy in the volume determination leads to a corresponding improvement in the accuracy of airbag pressure prediction. One of the important advantages of the finite element formulation is its ability to incorporate gas-dynamic models in the airbag inflation process. In airbag simulation, a gas inflation model is coupled to the airbag structure to describe the gas flow during inflation. The model is based on the assumptions that there is no heat transfer into the control volume, the gas is ideal with constant specific heats, and that the temperature and pressure are uniform within the control volume.

A generalized analytical model of an airbag inflation system was developed by Wang and Nefske [5]. They documented the thermodynamic aspects of the model. The model accounts for tabular input of mass flow rate and gas temperature to represent the inflator, and for airbag material stretch and airbag gas leakage.

The gas leakage through both vents and porous bag material plays an important role in dissipating the energy of an airbag system. In general, the more energy dissipated the less occupant rebound will be. However an excess of gas leakage can also result in insufficient bag pressure which may cause an unexpected occupant interaction with vehicle interior structures during a crash. Wang and Tung [6] quantified the energy dissipation capability of an airbag system.

There has been an extensive use of finite element codes in the simulation of airbag deployment. The purpose of the simulations has been to predict occupant loads, acceleration levels, and other severity measures that can help identify the effectiveness provided by the airbag system. Wawa et al. [7] validated the finite element airbag computational model with experimental results. Lakshminarayan and Lasry [8], and Khalil [9] have reported numerical simulations of the airbag-occupant interactions using the finite element method.

Apart from the automotive industry, research on occupant simulation is being conducted in the aerospace industry to investigate the possibility of incorporating airbags in aircraft and helicopters. The idea is to provide maximum protection to the pilot and navigator during collision against trees, stationary objects or crashes into large bodies of water. As in cars, deployment time for different folding configurations and various airbag parameters are of interest. The aim here is to achieve desirable deceleration and energy absorption of the air vehicle upon impact to maintain structural integrity. Multi-airbag systems consisting of airbags

deployable on the sides and ceiling have recently been introduced in automobiles for better protection of occupants during lateral as well as frontal impacts. Avula and Kaleps [10] have reported on the behavior of multi-airbag systems for optimal protection in the interior of helicopters and other military vehicles.

In the present work, an attempt has been made to simulate the behavior of an airbag attached to an air vehicle falling into water from an initial folded configuration, and capture the interaction of the airbag during its unfolding and subsequent contact with the water surface. A review of literature indicates that studies have not been conducted to test the effect of contact of the airbag with the water surface. In this work, a parametric investigation is carried out to study the effects on the evolution of pressure, volume and temperature within the airbag when the airbag impacts a water surface. Also, the effect of material properties and the vent diameter on the airbag is studied.

II. AIRBAG MODELING

An airbag essentially consists of a fabric bag and an inflator which has to produce the gas needed to inflate the bag. In designing a pyrotechnic airbag inflator the heat transfer, filtration, combustion, fluid flow and thermodynamic processes occurring during the inflation are to be considered.

There are generally three important aspects to the modeling of airbags: (1) the modeling of the airbag fabric, (2) modeling of the interior of the airbag using control volume approach, and (3) the equation of state that provides the gas pressure as a function of temperature and density.

The fabric of the airbag is characterized by a composite orthotropic elastic material model described in LS-DYNA3D manual [11]. These fabrics exhibit a strong material nonlinearity and tend to buckle because they cannot sustain compressive and bending stresses. An additional complicating factor is that the fibers in the fabric interact in a complex manner that can deviate considerably from the continuum behavior. In LS-DYNA3D, the approach described by Lloyd [12] for treating nonlinear fabric behavior is followed. The airbag fabric model is based on an orthotropic elastic material model, which can be used in conjunction with several shell elements. To allow for an arbitrary orientation of the finite elements within the mesh, each ply in the fabric may have a unique orientation angle that can be defined at each integration point through the laminate thickness. In the implementation of the material model, the transformation is first carried out on the Cauchy stress tensor σ and the rate of deformation tensor \mathbf{d} with the material coordinate system denoted by the subscript L. Then the stress state is incrementally updated in the material coordinates by:

$$\sigma_{L}^{n+1} = \sigma_{L}^n + \Delta \sigma_{L}^{n+\frac{1}{2}} \quad (1)$$

where,

$$\Delta \sigma_L^{n+\frac{1}{2}} = \begin{bmatrix} \Delta \sigma_{11} \\ \Delta \sigma_{22} \\ \Delta \sigma_{12} \\ \Delta \sigma_{23} \\ \Delta \sigma_{31} \end{bmatrix} = \begin{bmatrix} Q_{11} & Q_{12} & 0 & 0 & 0 \\ Q_{12} & Q_{22} & 0 & 0 & 0 \\ 0 & 0 & Q_{44} & 0 & 0 \\ 0 & 0 & 0 & Q_{55} & 0 \\ 0 & 0 & 0 & 0 & Q_{66} \end{bmatrix} \begin{bmatrix} d_{11} \\ d_{22} \\ d_{12} \\ d_{23} \\ d_{31} \end{bmatrix} \Delta t. \quad (2)$$

The terms Q_{ij} are defined as follows

$$Q_{11} = \frac{E_{11}}{1 - \nu_{12}\nu_{21}}, Q_{22} = \frac{E_{22}}{1 - \nu_{12}\nu_{21}}, Q_{12} = \frac{\nu_{12}E_{11}}{1 - \nu_{12}\nu_{21}}, Q_{44} = G_{12}, Q_{55} = G_{23}, Q_{66} = G_{31} \quad (3)$$

Because of the symmetry properties

$$\nu_{21} = \nu_{12} \frac{E_{22}}{E_{11}} \quad (4)$$

Also, thermodynamic considerations require the following constraints to be enforced at each time step

$$|\nu_{12}| < \sqrt{\frac{E_2}{E_1}} \quad |\nu_{21}| < \sqrt{\frac{E_1}{E_2}} \quad (5)$$

The fabric material model differs from an elastic orthotropic model in two important ways

1. Compressive stresses are inadmissible, and
2. There exists an initial slack, i.e., only low levels of stresses are developed in the fibers until the material is stretched taut.

This behavior can be modeled by representing the modulus of the fiber as a function of fiber strain. The zero compressive modulus simulates the slack in the fabric.

Five material parameters are used in the three failure criteria. These are: S_1 , longitudinal tensile strength; S_2 , transverse tensile strength; S_{12} , shear strength; C_2 , transverse compressive strength; α , nonlinear shear stress parameter.

S_1 , S_2 , S_{12} , C_2 are obtained from material strength measurement. α is defined by material shear stress-strain measurements. In the plane stress, the strain is given in terms of the stress as

$$\varepsilon_1 = \frac{1}{E_1} (\sigma_1 - \nu_1 \sigma_2) \quad (6)$$

$$\varepsilon_2 = \frac{1}{E_2}(\sigma_2 - \nu_2 \sigma_1) \quad (7)$$

$$2 \varepsilon_{12} = \frac{1}{G_{12}} \tau_{12} + \alpha \tau_{12}^3 \quad (8)$$

Equation (8) defines the nonlinear shear stress parameter α . A fiber matrix shearing term augments each damage mode

$$\bar{\tau} = \frac{\frac{\tau_{12}^2}{2G_{12}} + \frac{3}{4}\alpha\tau_{12}^4}{\frac{S_{12}^2}{2G_{12}} + \frac{3}{4}\alpha S_{12}^4} \quad (9)$$

which is the ratio of the shear stress to the shear strength.

The matrix cracking failure criteria is determined from

$$F_{matrix} = \left(\frac{\sigma_2}{S_2} \right)^2 + \bar{\tau} \quad (10)$$

where failure is assumed whenever $F_{matrix} > 1$. If $F_{matrix} > 1$, then the material constants E_2 , G_{12} , ν_1 and ν_2 are set to zero.

The final failure model is due to fiber breakage.

$$F_{fiber} = \left(\frac{\sigma_1}{S_1} \right)^2 + \bar{\tau} \quad (11)$$

Failure is assumed whenever $F_{fiber} > 1$. If $F_{fiber} > 1$, then the material constants E_1 , E_2 , G_{12} , ν_1 and ν_2 are set to zero. The fabric material model considered for the analysis is composed of several layers of the above-mentioned material model.

Control Volume Modeling: A direct approach for modeling the contents of the airbag would be to discretize the interior of the airbag using solid elements. The total volume and pressure-volume relation of the airbag would then be the sum of all elemental contributions. Although this direct approach could be applied in a straight forward manner to an inflated airbag, it would become very difficult to implement during the inflation phase of the airbag deployment. Additionally, as the model is refined, the solid elements would quickly overwhelm all other computational modes and make the numerical simulation prohibitively expensive and time consuming.

An alternate approach for calculating the airbag volume, that is both applicable during the inflation phase and less computationally demanding, treats airbag as a control volume. The control volume is defined as the volume enclosed by a surface. In the present case the control surface that defines the control volume is the surface modeled by membrane elements comprising the airbag fabric material.

Because the evolution of the control surface is known, i.e., the position, orientation and current surface area of the airbag elements, we can take advantage of these properties of the control surface to calculate the control volume by applying green's theorem. This leads to:

$$V = \int xn_x dT = \sum_{i=1}^N \bar{x}_i n_{ix} A_i \quad (12)$$

where, V = control volume

N = number of elements

\bar{x} = average x coordinate for each element i

n_{ix} = direction cosine between the element normal and the x coordinate

A_i = the surface area of the element

The previous equation is implemented in DYNA3D with the direction of integration chosen to be parallel to the maximum principal moment of inertia of the surface. Numerical experiments have shown that this choice of integration direction produces more accurate volume than in selecting a coordinate direction or other principal inertia directions. A special treatment was also included to account for airbag venting holes.

At each time step in the calculation, the pressure in the airbag corresponding to the control volume can be determined from an equation of state (EOS) that relates the pressure to the current gas density (volume) and the specific internal energy of the gas. The EOS for the airbag simulation is the usual 'Gamma Law gas Equation of State' referenced in [11] which follows from thermodynamic considerations of adiabatic expansion of an ideal gas. This equation can be written as

$$P = (\gamma - 1) \rho e \quad (13)$$

where P is the pressure, γ is the ratio of specific heats, ρ is the density and e is the specific internal energy of the gas. The specific internal energy evolution equation corresponding to two states is given by

$$e_2 = e_1 [v_2 / v_1]^{(1-\gamma)}. \quad (14)$$

The control volume equation together with the EOS and the specific internal energy equation completely defines pressure-volume relation for an inflated airbag.

III. SIMULATION OF AIRBAG DEPLOYMENT ON WATER SURFACE

The simulation of the impact between an airbag and a body of water is carried out using the explicit nonlinear finite element program LS-DYNA3D. The pre-processing of the airbag and the body of water is done using LS-INGRID mesh generator. The processing was done in LS-DYNA3D. The post-processing of the output data is done in LS-TAURUS.

The input file to LS-INGRID contains the airbag characterization with its fold definitions and that of the water surface. The fabric material model of the material type 34 of LS-DYNA3D is chosen. This model is similar to the orthotropic composite material model. It is designed to allow a fabric to be modeled as a layered orthotropic material. The principal characteristic of a fabric material is that it does not support compressive stresses. This is because it is usually modeled with elements that are at least an order-of-magnitude wider than the thickness of the material. The numerical values given in the software example files of LS-DYNA3D [11] are used for the material and geometric parameters of the fabric and they are presented in Table I.

TABLE I: Material properties for the airbag fabric

Parameter	Variable	Units	Value
Thickness	t	Mm	0.35
Density	ρ_{fabric}	kg/m ³	1000
Young's Modulus	E	N/m ²	1.0x10 ⁰⁸
Poisson's Ratio	ν	-	0.4

The airbag folding pattern is generated in LS-INGRID mesh generator. The airbag is initially meshed as two separate layers. The location of fold lines, direction of fold, folding radius and sequence of folds are specified in the input file. The nodal point locations are then checked to avoid element inter-penetrations after folding. A series of thick folds are defined in the folding operation. The airbag model contains 1496 quadrilateral membrane elements. The orientation of bottom fabric layer is at 0° and 90°. For the top layer the orientation is -45° and 45°, as in an actual bag.

An equation of state based on the control volume approach in the Wang-Nefske airbag model is used to model the thermodynamic behavior of the gas flow into the airbag. It is assumed that the gas behaves as an ideal gas, and the process is adiabatic, and that the pressure and the temperature are distributed uniformly throughout the control volume. The mass flow rate for the inflator model is specified. The material properties of the bag are presented in Table II.

TABLE II : Thermodynamic properties of the gas and ambient air.

Material	Parameter	Variable	Units	Value
Nitrogen	Specific heat at Constant Volume	C_v	J/kg ^o K	741.0
	Specific heat at Constant Pressure	C_p	J/kg ^o K	1038.0
	Temperature	T	^o K	700.0
Air	Density	ρ_{air}	kg/m ³	1.0
	Ambient Pressure	P_e	Pa	1.0E05

The input gas temperature is considered to be constant with time. The mass outflow of the gas is defined by an exit hole coefficient of discharge and exit area. The volume occupied by the gas is internally monitored. From this volume of the occupied gas, the internal pressure is calculated using the equation

$$m_{out} = A\sqrt{2p\rho\mu}\sqrt{\frac{\gamma}{\gamma-1}\left[Q^{2/\gamma} - Q^{(\gamma+1)/\gamma}\right]} \quad (15)$$

where

$$Q = p_e/p \quad \gamma = c_p/c_v \quad p = (\gamma-1)E/V$$

m_{out} = Mass rate of the gas flowing out from the bag,
 c_v = Heat capacity at constant volume.
 c_p = Heat capacity at constant pressure.
 μ = Coefficient of discharge.
A = Exit area. p_e = Ambient Pressure.
 ρ = Ambient density. E = energy.
p = pressure. V = volume.

The calculated pressure would in turn be applied to the finite element model to obtain the new bag shape and volume. This interchange between the gas model and the finite element model provides the coupling between the two models.

For the three-dimensional contact-impact algorithm, one surface of the interface is identified as the master surface and the other as a slave. Each surface is defined by a set of three or four node quadrilateral segments, called master and slave segments, on which the nodes of the slave and master surfaces, respectively, must slide. Input for the

contact-impact algorithm requires that a list of master and slave segments be defined. For the single surface algorithm, only the slave surface is defined and each node in the surface is checked at each time step to ensure that it does not penetrate through the surface. Internal logic identifies a master segment for each slave node and a slave segment for each master node and updates this information every time step as the slave and master nodes slide along their respective surfaces.

A slideline is a contact algorithm to model the mechanical interaction between two bodies or two parts of the same body. As the airbag is inflated, surface folds come in contact with each other while unfolding. To eliminate the interpenetration between the surface nodes during inflation, an airbag single surface slideline algorithm, which is specially developed for airbags is used. For this a master surface need not be defined. The finite element model of the airbag closely represents the actual geometry of the airbag, and the physical phenomena associated with airbag dynamics such as bag deformation and contact.

To study the contact with the water surface, a body of water is modeled using the index space concept in LS-INGRID. An index space is commonly used for finite difference mesh generation. It is defined as a three-dimensional discrete coordinate system with integer values greater than or equal to 1 in each of the three directions. The three discrete coordinates are labeled, I, J and K axes respectively. Each point in the index space (i,j,k) , represents a nodal point. Elements are defined as groups of adjacent nodes in the index space. An enhancement to the three-dimensional index space is an additional type of index notion known as the Index Progression. Index progressions provide a concise and simple method for describing complex structures, and are used to input data to LS-INGRID. The node generation for the body of water has been done by mapping from Index space onto the object of interest, which generates a cube with brick elements. Part control commands are used to give the mesh the properties of water. In LS-INGRID there is no built-in material type to simulate the properties of water. To overcome this problem, a null material of material type 9 with an equation-of-state has been used to simulate the properties of water.

To study the contact between water surface and airbag, two types of approaches, viz., faceted contact entity approach and geometric contact entity approach are considered. Of these two, geometric contact entities require less storage and less computational time when compared to more general faceted contact entities. But the contact between two deformable bodies like airbag and water can be better simulated using the faceted contact entities for modeling. So in the present simulation faceted contact entity approach is used. This requires defining master and slave surfaces. The top surface of water body with 81 segments has been defined as the master surface. The entire airbag with 1496 segments is defined as a slave surface. Then an interface of type 3 in LS-INGRID i.e., sliding with voids contact is defined between master and slave surfaces. The dimensions of water body are made very large relative to those of the airbag. This is done because only the effects on the airbag are of interest in the present study. Finally, the simulation is carried out and the results are post-processed.

IV. RESULTS AND DISCUSSION

The evolution of pressure, volume and temperature by the parametric variations of material properties, vent size and the distance of airbag from the water surface are computed. The airbag validated by Avula, Kaleps and Mysore [13] is used for the simulation.

INTERACTION OF AIRBAG DEPLOYMENT WITH WATER SURFACE

The effect of variation of distance from which then airbag impacts the water surface is analyzed. Distance from which the airbag impacts the water is varied from 0.04m to 0.2m. Typical interaction profiles of an airbag inflating against the water surface from a distance of 0.08m at various times are shown in the Fig. 1. The evolutions of temperature, volume and pressure in an airbag impacting against a semi-infinite body of water are shown in Figs. 2, 3 and 4, respectively. From these figures it was observed that the impact of the airbag with water surface produces an increase in peak pressure in comparison with the airbag deployed in the absence of the water surface. (Results of airbag inflation in the absence of water surface are not shown here for brevity; these results are presented in [13]).

Effect of Airbag Distance From Water Surface

The evolution of peak pressure as a function of airbag distance from water surface is shown in Fig. 5. . Here it is observed that, when the airbag is close to the water surface, the resistance to the unfolding airbag is high and this results in higher peak pressure in the bag. As the distance of the airbag from water surface increases, the pressure becomes less because the resistance to the unfolding of airbag also becomes less. The trend continues up to a distance of 0.14m after which the pressure does not vary with distance. This constant pressure is attained because at the distance of 0.14m the bag is fully inflated even before it came in contact with the water surface, and as such there is no effect of water surface on the airbag. Thus, with increasing distance of airbag from the water surface, the pressure in the airbag first decreases and then becomes constant. Figures 6 and 7 show the peak volume and peak temperatures attained inside the airbag as a function of the distance of the airbag from the water surface. These figures show that the trend in case of temperature is similar to that of pressure. The volume attained in the airbag increases when the distance of airbag from the water surface increases. This is as expected because the gas inside the airbag obeys the gas law.

Effect of Fabric Density

To study the effect of fabric density on airbag deployment, a parametric study is carried out with airbag fabrics of densities ranging from 500 kg/m^2 to 15000 kg/m^2 . Two different cases, one with airbag deployed against the water surface and the other with

airbag expanding freely are considered. The comparison of the variation of computed peak pressures, peak volumes and peak temperatures within the bag for different values of fabric density for the two cases is shown in Figs. 8, 9 and 10. The pressure attained in the airbag of lower material fabric density is less in comparison with that for higher material fabric density. Thus, a high bag volume and the corresponding low bag pressure result for the lowest bag density airbag model, and there is almost a linear increase in the bag pressures and a linear decrease in bag volumes as the fabric density increases. The trend exhibited by the evolution of temperatures inside the airbag is similar to that exhibited by the pressures.

Effect of Vent Size

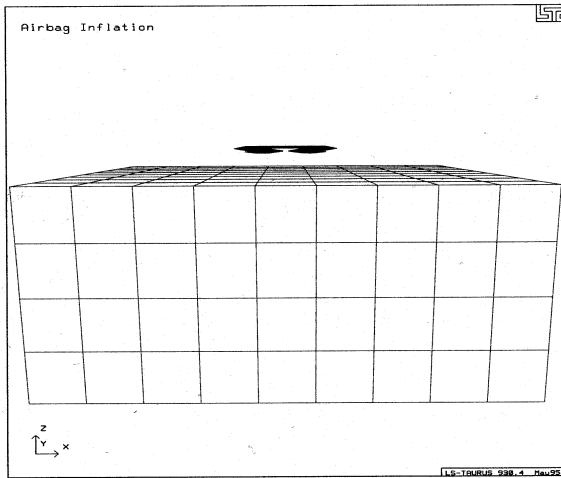
The effect of parametric variation in the vent size on the evolution of pressure, volume and temperature is studied. Different vent diameters ranging from 0 to 9.426 cm² are considered. In all the cases the coefficient of discharge of the vent hole is assumed to be 0.7. During the gas generation, the mass of gas flowing out of the bag is considered negligible in comparison with the mass of the gas flowing into the bag. As such the effect of the venting can be observed only after the gas generation is stopped. It is found that as the diameter of the vent hole decreases, the volume of the gas escaping from the airbag also decreases. This results in higher values of volume, pressure and temperature inside the airbag. The pressure, volume and temperature curves are identical until the gas generation inside the airbag stops after which the curves assume different paths depending on the vent diameter. These results are not shown for brevity. Observe the peak pressure, volume and temperature in Figs. 5, 6 and 7.

Effect Of Fabric Elasticity

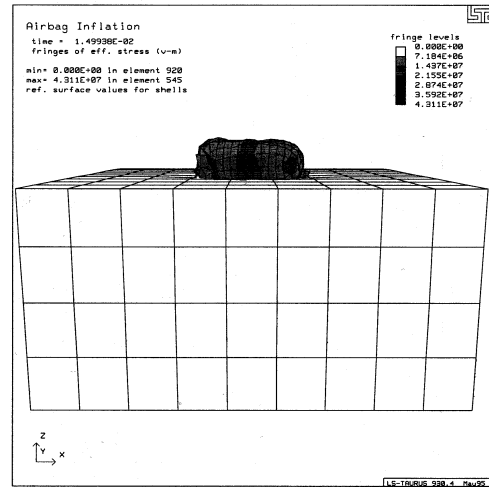
A parametric study is conducted to study the effect of the bag elasticity. Different values of the elastic modulus are used in the simulation. It is found that lower elastic modulus implies weaker bags and increased stretch. This bag stretch results in higher volumes in weak material bags and lower volumes in case of stiff material bags. Observation of pressure curves indicates that higher pressures result for bags with higher modulus of elasticity.

Effect of Gas Temperature

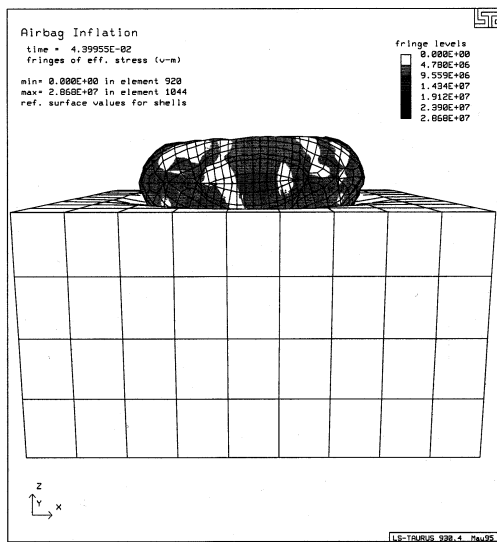
To consider the effect of variation of the input gas temperature on the evolution of pressure, volume and temperature, a parametric study is carried out. When the input gas temperature is very low, improper inflation of airbag occurs and this results in low bag volume. Airbag pressures and airbag volumes increase progressively with increase in the input gas temperatures.



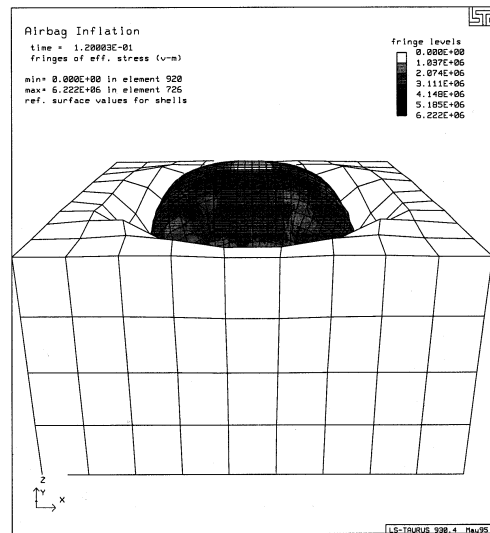
a) Before Inflation



b) Inflated airbag at 16 m sec



c) Inflated airbag at 45 m sec



d) Fully Inflated airbag

Figure 1. Inflation of airbag on water surface at various times

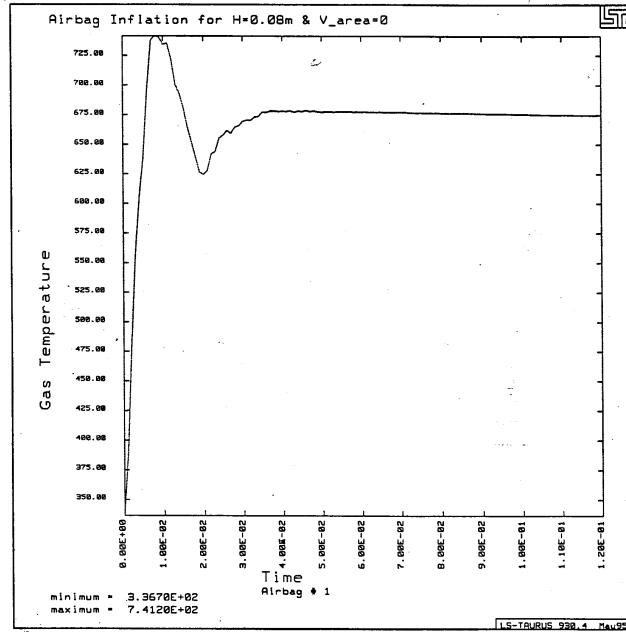


Figure 2. Temperature-time history of airbag inflating against the water surface

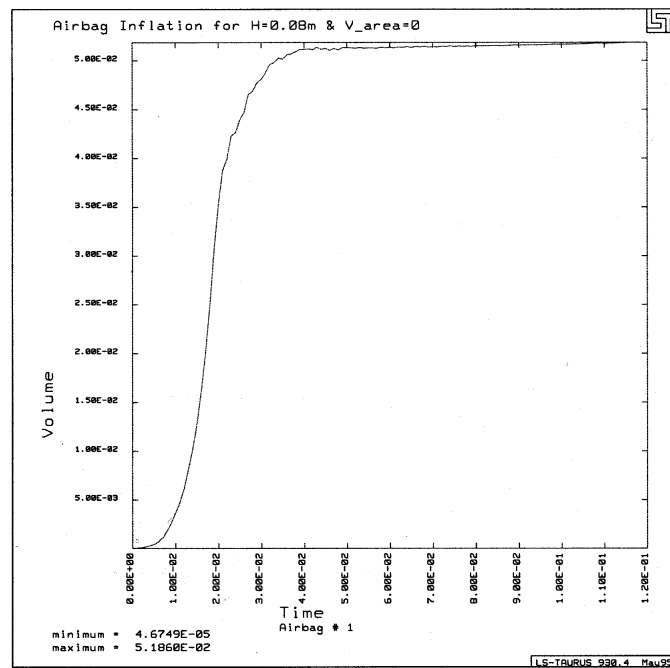


Figure 3. Volume-time history of airbag inflating against the water surface

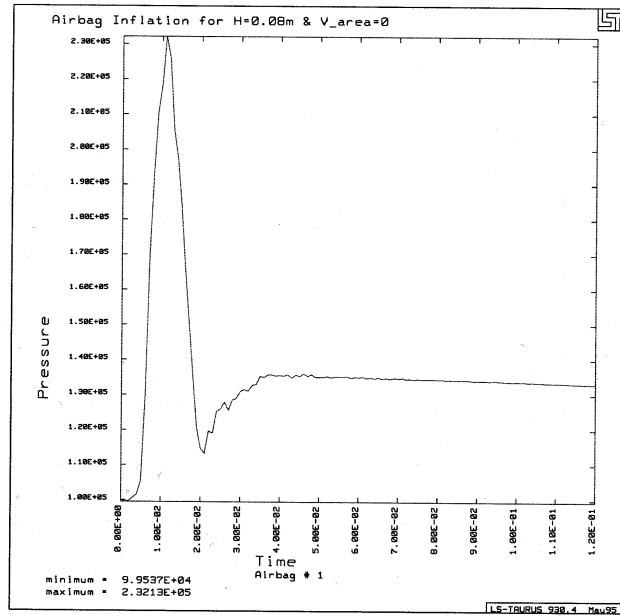


Figure 4. Pressure-time history of airbag inflating against the water surface

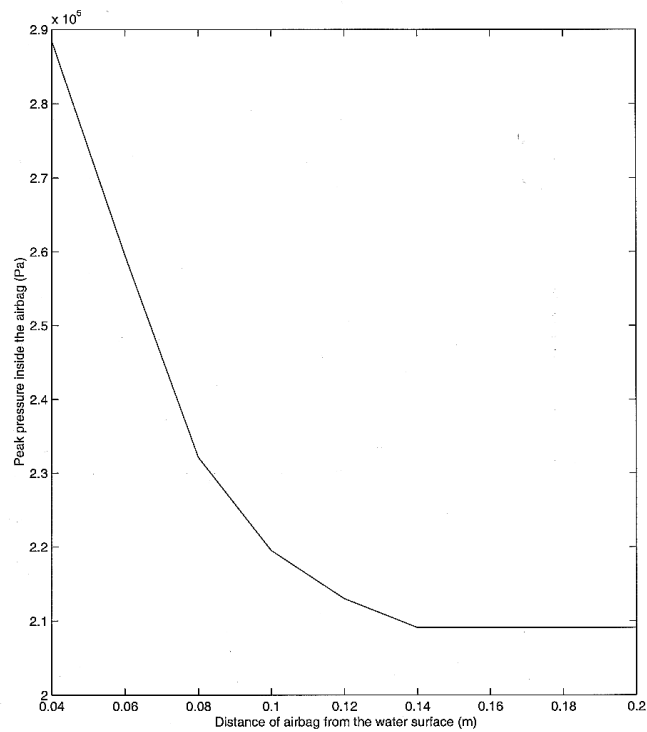


Figure 5. Peak pressures for an airbag with zero vent area as a function of distance from the water surface

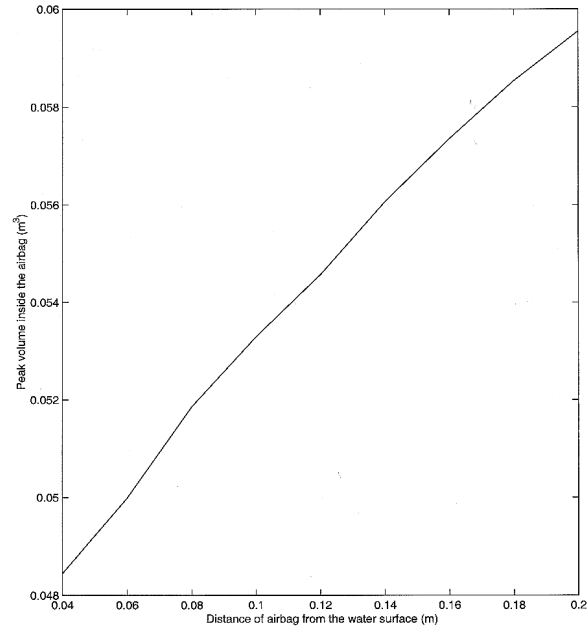


Figure 6. Peak volumes for an airbag with zero vent area as a function of distance from the water surface

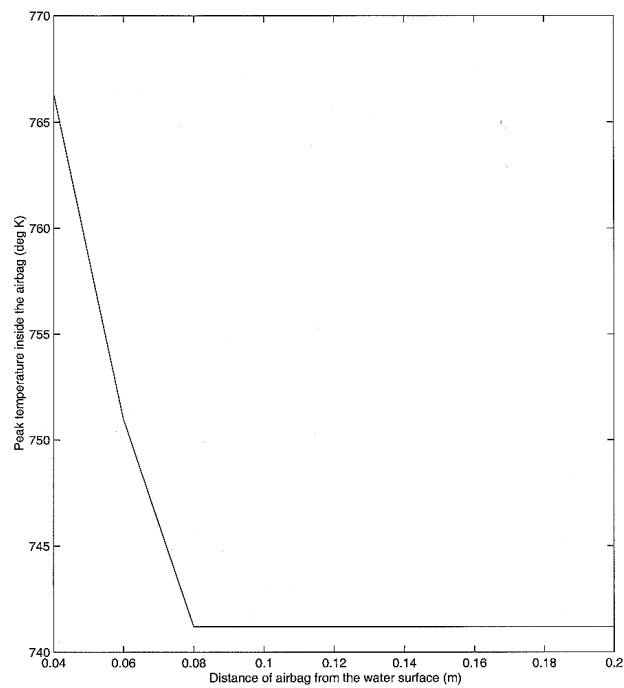


Figure 7. Peak temperatures for an airbag with zero vent area as a function of distance from the water surface

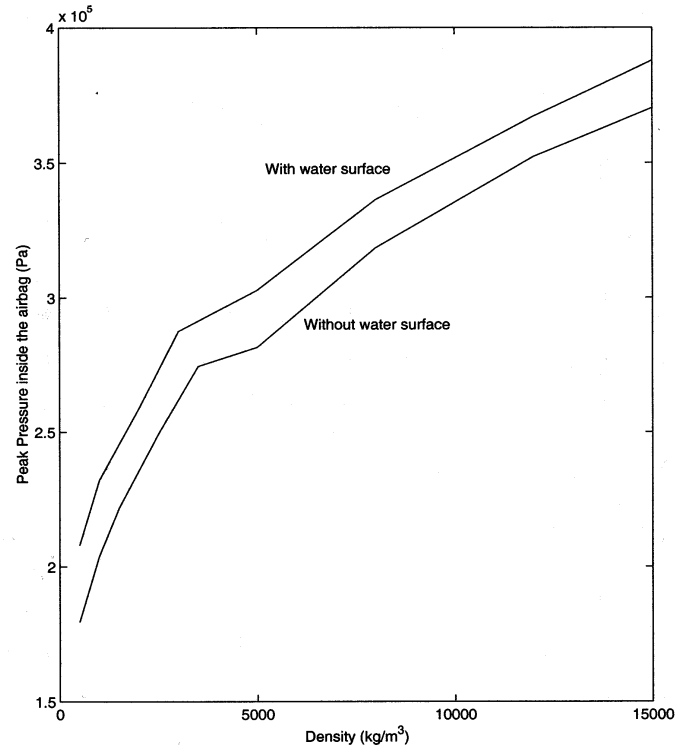


Figure 8. Comparison of peak pressures within the airbag as a function of fabric density

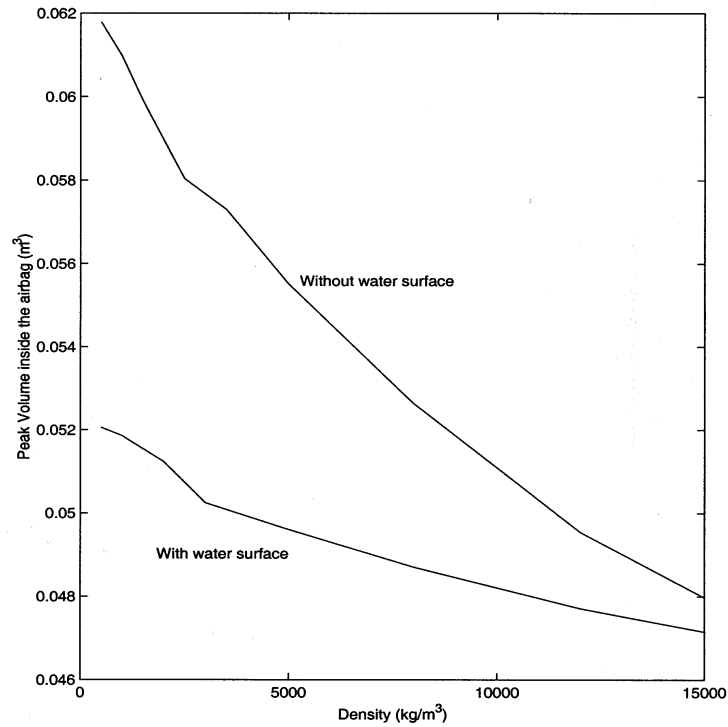


Figure 9. Comparison of peak volumes within the airbag as a function of fabric density

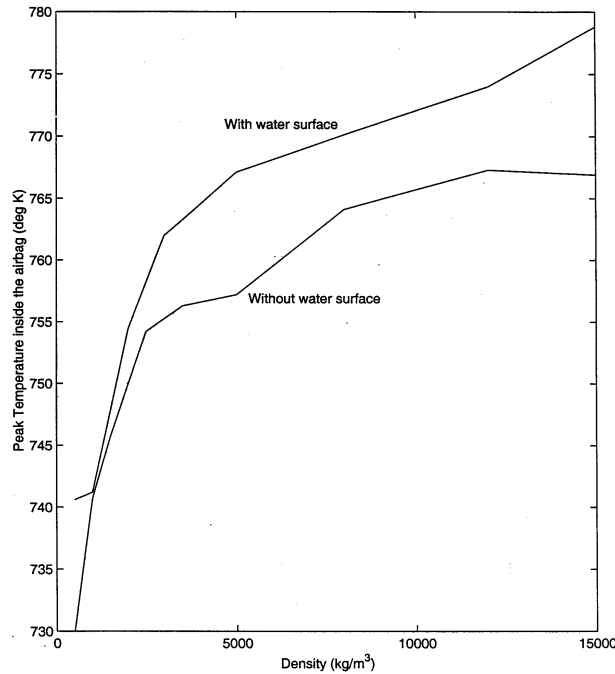


Figure 10. Comparison of peak temperatures within the airbag as a function of fabric density

BEHAVIOR OF AIRBAG ATTACHED TO A FALLING HELICOPTER

A conceptual scenario of an airbag deployed from the bottom of a disabled helicopter falling into water is shown in Fig. 11.

In this section, an airbag attached to the base of a solid body falling into water is treated. This situation arises when an aircraft or a helicopter loses power during combat or rescue operations at sea and falls freely into water. The motivation behind this simulation is to study the feasibility of using airbags as protective devices, to prevent damage to the structure and the occupants of flying vehicles such as helicopters and airplanes. In the example considered the weight of a 40,000 N helicopter is distributed over the top surface of the airbag. The helicopter is assumed to be freely falling when it crashes into water. The height from which it is falling on to the water surface is varied from 1.25m to 5m. Based on the conservation of energy principle, this height (h) is converted into the velocity (v) using the formula $v^2 = 2gh$. This velocity is in turn applied to the 1296 nodes on the top surface of the airbag. This velocity is assumed to follow a load curve which decreases exponentially from an initial value of 10m/s to a final value of zero because of the resistance offered by the airbag. The effects of the crash on the bag pressure, volume and temperature are shown in Figs. 12, 13 and 14. Figure 15 shows the variation of the peak pressure of the airbag with the height from which the helicopter falls. This figure shows that with an increase in the distance from which the helicopter crashes, there is a corresponding increase in the peak pressures of the airbag. In Figure 16



Figure 11. Conceptual scenario of helicopter falling into water protected by an airbag

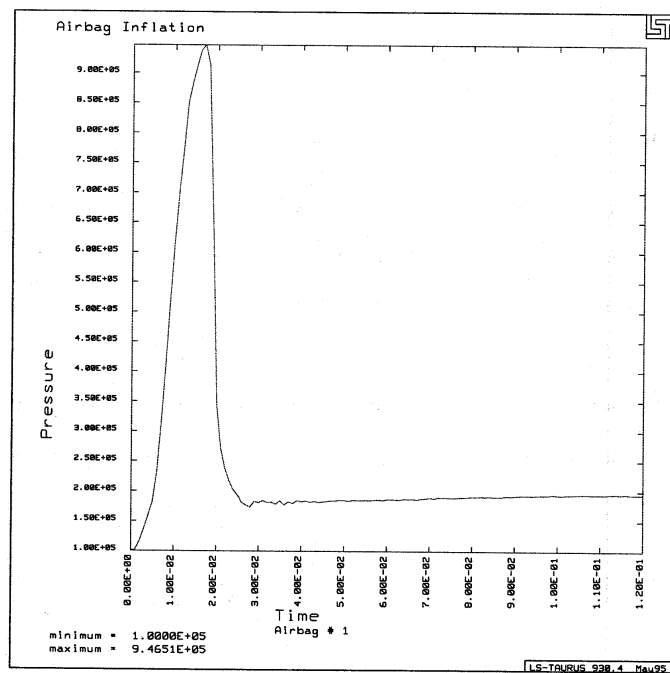


Figure 12. Pressure-time history of airbag deployed under a falling helicopter

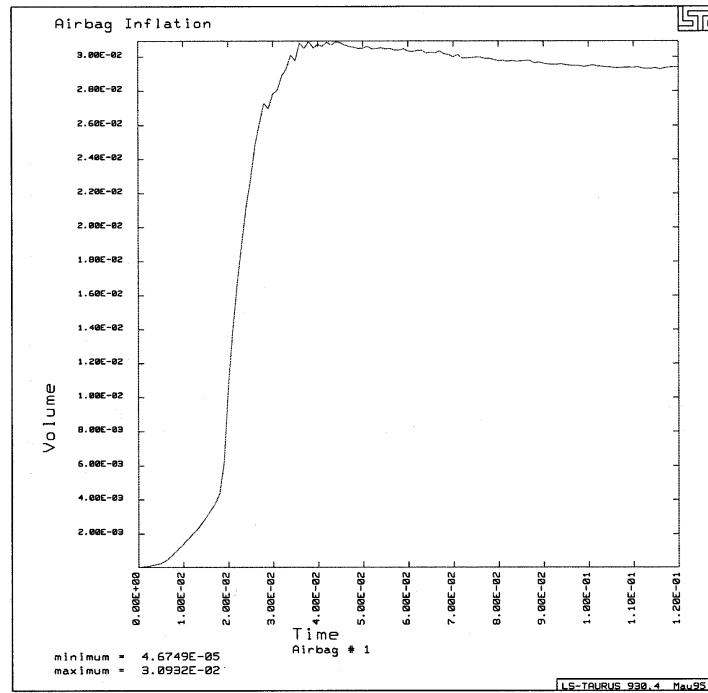


Figure 13. Volume-time history of airbag deployed under a falling helicopter

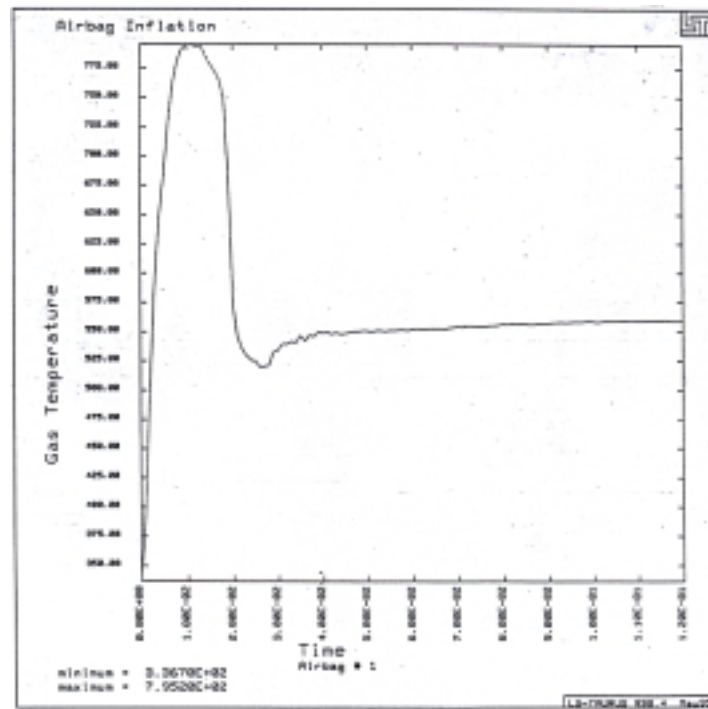


Figure 14. Temperature-time history of airbag deployed under a falling helicopter

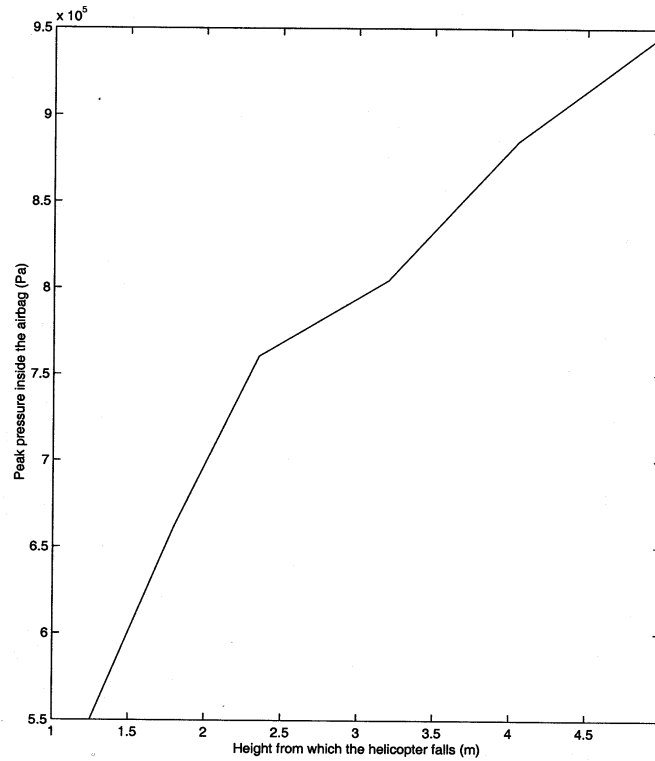


Figure 15. Peak pressures within the airbag as a function of height from which the helicopter falls

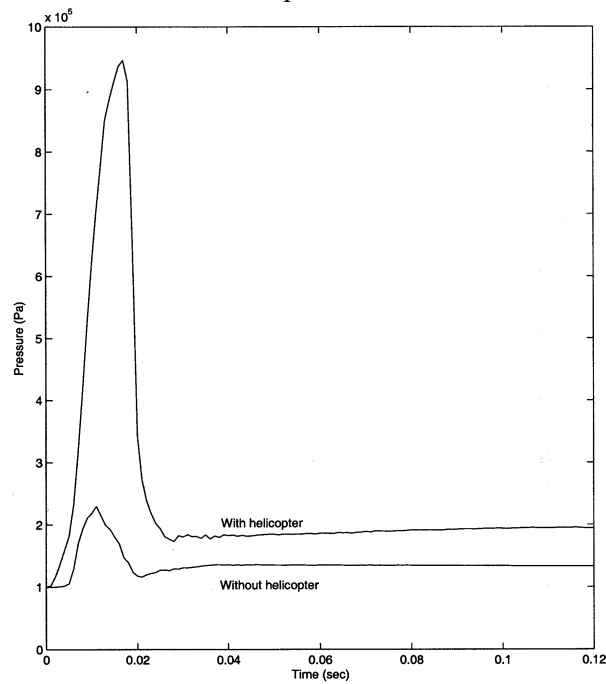


Figure 16. Comparison of pressure-time histories for an airbag with and without attachment to helicopter

the variation of the airbag pressure when it is deployed underneath a falling helicopter is compared with the variation in bag pressure when airbag is not attached to the helicopter. From this graph it is clear that there is a steep increase in the airbag pressures when the vertical velocity of the helicopter is imposed on the airbag.

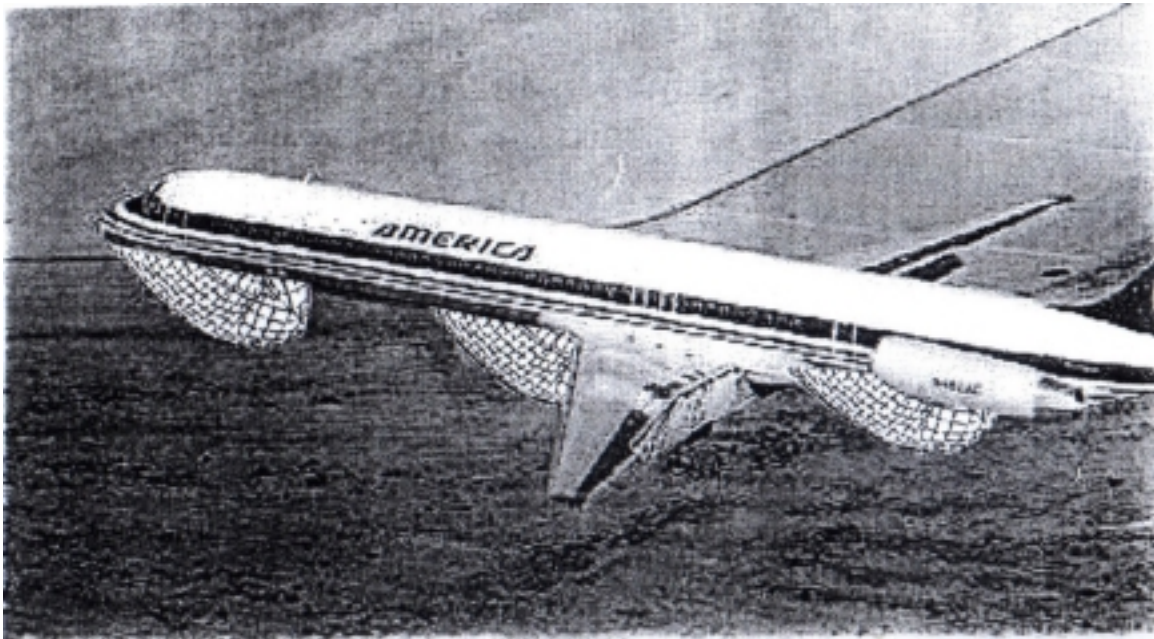


Figure 17. Possible scenario of multiple airbags deployed under a disabled aircraft

FUTURE APPLICATIONS

A scenario of multiple airbags deployed at the bottom of a disabled aircraft landing on water (or, on hard surface) is presented in Fig. 17. This is a difficult situation to analyze at this time for lack of appropriate design parameters and material requirements. However, the idea is presented for possible future investigation.

V. CONCLUSIONS

In this study a computer simulation of the deployment of an initially folded airbag and its impact with a water surface is performed using the nonlinear finite element program LS-DYNA3D.

To validate the program, the airbag is first deployed and allowed to inflate freely without any water surface. A comparison of the simulation of the unfolding process with experimental test results reported in literature has shown good agreement.

When the airbag is inflated from different initial positions above the water surface, practically no difference in the unfolding timings of airbag is observed from the timings of the airbag deployed without water surface. When an airbag is attached to the base of a freely falling body such as a disabled helicopter and deployed against the water surface, there exists an optimal distance from which the airbag has to be deployed against the water surface for highest protection.

A parametric study is conducted to investigate the influence of airbag parameters on the evolution of pressure, volume and temperature within the airbag when it is inflated against the water surface. Various airbag parameters including venting, fabric density, fabric elasticity and input gas temperature are considered. It is observed that low input gas temperature resulted in improper inflation of the airbag. Higher fabric densities significantly increased the ability of airbag to withstand higher pressures. Also, it is inferred that higher bag elasticities are required to make stiff material bags which can withstand higher pressures involved in helicopter crashes. Though the ability of the bags to withstand higher pressures is an important criteria, the chief purpose of an airbag is to prevent injury to the occupants and damage to the structure during a crash. So a recommendation is made to strike a balance between various airbag parameters such that airbag could withstand higher pressures and at the same time should offer less rebound to the structure and the occupants.

REFERENCES

- [1] Coltman, J.W., Arndt, S., Domzalski, L., Evaluation of the Crash Environment and Injury-causing Hazards in U.S Navy Helicopters, SAFE Journal-Vol. 16, No.1, 1986.
- [2] Alem, N.M., Shanahan, D.F., Barson, J.V., Muzzy, W.H., The Effectiveness of Airbags in Reducing the Severity of Head Injury From Gunsight Strikes in Attack Helicopters. AGARD CP-532, Neuilly-sur-Seine, France, 1992.
- [3] Shahanan, D.F., Shanon, S.G., Bruckart, J.E., Projected Effectiveness of Airbag Supplemental Restraint Systems in US Army Helicopter Cockpits, USSARL Report No. 93-31, September 1993.
- [4] Crowley, J.S. and Dalgard, C.L. (Eds.) Proceedings of the Technical Cooperative Program Workshop: Inflatable Restraints in Aviation, U.S. Army Aeromedical Research Laboratory Report No. 2000-21, August 2000.
- [5] Wang, J. T., J. D. Nefske, A New CAL3D Airbag Inflation Model, SAE Paper No.880654, 1988.
- [6] Wang, J.T. and Tung, D.B., A Procedure for Quantifying the Effect of Leak Area of a Full Size Airbag, SAE Paper No. 970577, 1977.

- [7] Wawa, J. C., S. J. Chandra, K. M. Verma, Implementation and Validation of a Finite Element Approach to Simulate Occupant Crashes with Airbags: Part I – Airbag Model, AMD-Vol. 69/BED-Vol. 25, Crash worthiness and Occupant Protection Systems, ASME 1993.
- [8] Lakshminarayan, V. and D. Lasry, Finite Element Simulation of Driver Folded Airbag Deployment, SAE Paper No.912904, 1991.
- [9] Khalil, T. B., R. J. Wasko, J. O. Hallquist, D. W. Stillman, Development of a 3-Dimensional Finite Element Model of Air Bag Deployment and Interactions with an Occupant Using DYNA3D, SAE Paper No.912906, 1991.
- [10] Avula, X.J.R. and Kaleps, I., Modeling Multi-Airbag Systems for Optimal Protection, U.S. Army Aeromedical Research Laboratory Report No. 2000-21, Proceedings of the Technical Cooperative Program Workshop: Inflatable Restraints in Aviation, J.S. Crowley and C.L. Dalgard, Eds., pp. 121-130, May 2000.
- [11] LS-INGRID Theoretical Manual, Livermore Software Techn. Corp., 1994.
- [12] Lloyd, D. W., The Analysis of Complex Fabric Deformations, in Hearle. J. W. S., et al. Eds., Mechanics of Flexible Fibers Assemblies, Sijthoff & Noordhoff, The Netherlands, 1980.
- [13] Avula, X.J.R, Kaleps, I. and Mysore, G., Forces and Deformed Configurations of Airbag During Inflation and Impact, NATO-RTO-MP20, pp. 12-1 to 12-14, August 1999.